Automatic Circulating Tumor Cell Segmentation and Enumeration in Digital Pathology by Using Deep Learning and Ball-scale Based Filtering Techniques

L. Tong[1] and Y. Wan[2]

1. Conestoga High School, Berwyn, Pennsylvania, USA
2. Biomedical Engineering Department, Binghamton University, New York, USA
tripletonytong@gmail.com, ywan@binghamton.edu

Circulating tumor cells (CTCs) shed from the primary tumor, intravasate into blood, and translocate to distant tissues via circulation [1]. CTC enumeration allows cancer detection, treatment monitoring, and survival prediction [2, 3]. In the clinical setting immunofluorescence-based CTC enumeration is primarily used by expert cytopathologists. Manual enumeration requires cytopathologists with rich experience to read hundreds to thousands of images in hours. Despite the seemingly high number, this poor efficiency hinders the relevant clinical implementation. Therefore, high-automation enumeration is missing but highly desired [4]. Here, we proposed an automatic CTC segmentation and enumeration method in digital pathology by using deep learning techniques. To prepare for enumeration, peripheral blood mononuclear cells (PBMC) were extracted from cancer patient blood followed by infection with a reengineered adenovirus, *i.e.*, rAd^{CTC}, which is a CD46-targeting, DF3 promoter-selective, and GFP-overexpression adenovirus. The rAd^{CTC} ensures detection specificity and efficiency of expression for CTCs. Subsequently, PBMCs were stained with anti-CD45 fluorescence-labeled antibody and DNA staining dye DAPI. Finally, the acquired fluorescence images were used for automatic segmentation and enumeration [5]. It is noteworthy that the fluorescence images used in this study contain three channels. The green, red, and blue signals respectively represent overexpressed GFP in infected cells, CD45 staining on leukocyte membranes, and nuclear staining.

Table 1. Dataset (Image) Distribution

Data sets	Detection	Segmentation	Enumeration
Training	233 images	236 images	198 images (323 CTCs)
Validation	93 images	95 images	
Testing	140 images	142 images	
Total	466 images	473 images	
Size	1280×1080×3	64×64×3	1280×1080×3

U-Net is a convolution neural network (CNN) variant that has been widely used in biomedical image segmentation [6]. CNN tools were applied to count cell number in [7] and [8]. However, it is not clear what kind of useful features were extracted in the procedure and how much expert knowledge can affect or improve the cell counting. Thus, in this study, we investigated CTC counting by combining deep learning via U-Net and prior human knowledge of CTCs from ball-scale (B-scale) filter, which essentially provides the circular size of a cell [9], and proposed an automatic CTC enumeration approach from the fluorescence images. Figure 1 shows the flow of the model following expert cytopathologist behavior in counting CTCs: i) to detect or recognize the nuclei regions which provide the region-of-interests (ROI) for segmentation; ii) to focus on ROIs and segment or delineate the cell boundary; and iii) to further discriminate CTCs by reducing the false positive (FP) nuclei and finally count CTC number. In order to mimic this expert cytopathologist behavior, we designed two separate U- Nets for detection and segmentation. Table 1 lists all image datasets (in 3 channels). We first proposed a nuclear center-point based ROI detection approach by using U-Net. The ROI was determined by the location of the center-point (x_c, y_c) as well as the horizontal and vertical distance offset $(\Delta x_{TL}, \Delta y_{TL}, \Delta x_{BR}, \Delta y_{BR})$ between the center-point and top-left and bottom-right points as show in Figure 2. The network architecture (using green channel as an example) is shown in Figure 3. We replaced the de- convolutional layer with an up-sampling layer for reducing the number of parameters. 3x3 kernels and 32 output channels (in the middle of U-Net) can reduce the redundancy of the feature pyramid.

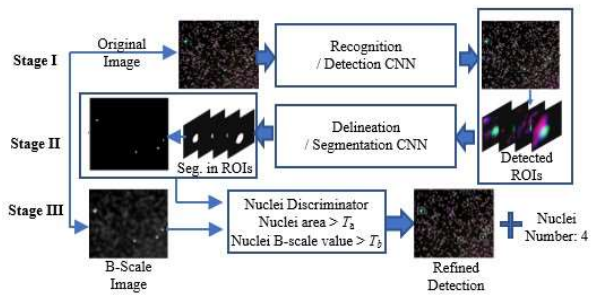

Figure 1. The flowchart of the proposed approach.

The loss function for our network is expressed as follows:

$$L(S_G, O_G; W) = -\frac{1}{N}\sum_{x\in\Omega} \log(P(l = S_G(x)|x)) + \frac{\lambda_1}{N}\sum_{x\in\Omega} \|O_G(x) - O(x)\|_1 + \lambda_2 \|W\|_1 \quad (1)$$

where $S_G(x)$ and $O_G(x)$ denote the ground truth of the category and distance offset at pixel x, $P(l = S_G(x)|x)$ represents the possibility value of pixel x classified as ground truth $S_G(x)$, $O(x)$ denotes the predicted distance offset at pixel x, W and Ω represent the parameters of the network and image domains, $\|\cdot\|_1$ is the L1-norm, and λ_1 and λ_2 serve as trade-off parameters among the three terms. Segmentation network follows the similar architecture as detection but using the cropped tumor cell masks as training samples. The loss function is the FP (false positive) &FN (false negative) +DICE loss function.

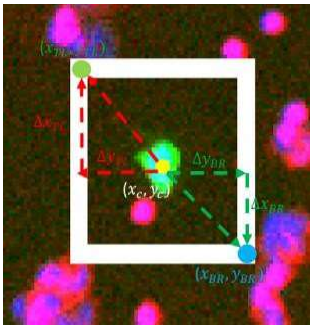

Figure 2. Center-point based ROI.

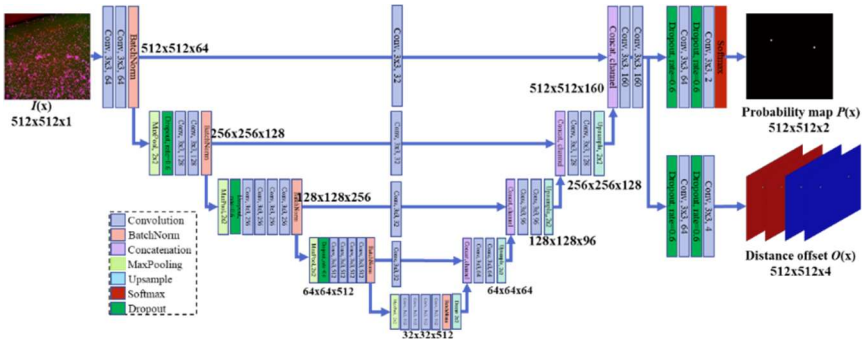

Figure 3. The architecture of the detection network.

B-scale based filter was originally developed for organ and tissue segmentations in MRI and CT [9,10]. We are the first to adopt it into digital pathology according to our knowledge. The significance of b-scale is that the pixel value in a B-scale image is returned as the maximum ball radius for that pixel (according to the homogeneity defined inside the ball [10]), thus giving us the relative size of the cell. B-scale provides the information that allows us to enhance the image by coding the size (ball radius) and the object shape (similarity to a ball) information which can and then be used in the discriminator steps as shown in Figure 1, where the area of cell segmentation and the B-scale value at each pixel were used together to set up a joint threshold/ criteria (using training data set) to reduce the false positive rate of nuclei detection and facilitate the cell counting to a better degree of success.

Table 2. CTC Segmentation Performance on Testing Set

Methods	Detection		Segmentation	Enumeration
	Precision	Recall	DICE	Missing rate
Proposed	0.98/0.10	0.92/0.18	0.85/0.08	0.04
Threshold	0.82/0.15	0.96/0.13	0.69/0.14	0.30

We thus reported the quantitative results for detection, segmentation and cell enumeration as shown in Table 2. Precision and Recall were two common factors used for evaluating detection results in pattern recognition; in addition, we also used the 2D Dice index (DICE) to evaluate the nuclei segmentation performance. The missing rate for CTC counting (FN/(TP + FN)) on all testing images was 0.04. Without using B-scale in the discriminator, interestingly, the missing rate was 0.09. To compare with our method, we ran another test using a strict threshold only method on the green channel. The result is listed alongside the b-scale method results in Table 2. This threshold was obtained based on the experiment on a subset of training samples using grid search. The threshold which gave the smallest sum of the false positive ratio and false negative ratio for tumor cell segmentation in relation to the ground truth was picked. Results show that our method is much better than that with a missing rate comparison of 0.04 to 0.30. Our method is also much comparable with the results in the most recent publication [7], which reported sensitivity and specificity as around 0.95 and 0.92 respectively, but required a significantly larger training data set. Despite this, we still achieved a similar true positive rate (recall vs. sensitivity). Currently, one of our only limitations is that we did not have the ground truth number of all non-tumor cells which need more efforts

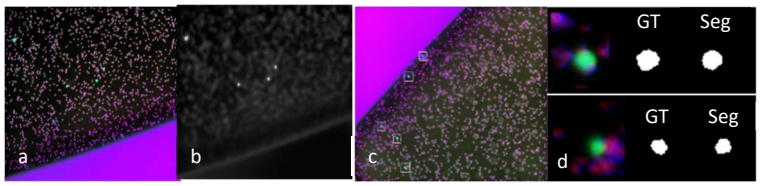

Figure 4. The B-Scale filter on the original image (a) with the enhanced image (b); delineation and segmentation samples are in (c) and (d).

to count and enumerate all non-tumor cells into ground truths. Although we have the number of false positive cases, we thus cannot report true negative ratio (specificity). But as we have observed, our CTCs are much less in number than the present non-tumor cells, so our false positive cases are actually very small, and the true negative ratio can be deduced to be very high. Figure 4 shows the visual results from the B-scale filter method, detection, and segmentation. Figure 4 (b) shows the B-Scale enhanced image which significantly suppresses the noise in the green channel of(a). Figure 4 (c) shows the ROIs from U-Net, and Figure (d) shows the segmentation samples compared to the Ground truth (GT) images. An Ubuntu (18.04) system PC with two NVIDIA 1080Ti GPUs with RAM of 11Gbytes was the PC system we used to conduct our experiments. One GPU was used to train the detection network for 500 epochs costing 6 hours and another one to train the segmentation network using cropped samples for 1000 epochs costing 40 minutes.

In this study, we proposed an automatic circulating tumor cell segmentation and enumeration in digital pathology through using deep learning and B-scale based filtering techniques. The proposed approach can get much comparable results with the current methods in literatures with a limited training data set. We will continue to improve the algorithm by involving more data sets and optimizing network architecture in the future.

ACKNOWLEDGEMENTS

The research reported in this paper is supported by a grant from the National Cancer Institute 1R37255948.

REFERENCES

[1] S. J. Hao, Y. Wan, Y. Q. Xia, X. Zou, and S. Y. Zheng, "Size-based separation methods of circulating tumor cells," Adv Drug Deliv Rev, vol. 125, pp. 3-20, Feb 1 2018.

[2] N. Aceto, A. Bardia, D. T. Miyamoto, M. C. Donaldson, B. S. Wittner, J. A. Spencer, et al., "Circulating tumor cell clusters are oligoclonal precursors of breast cancer metastasis," Cell, vol. 158, pp. 1110-1122, Aug 28 2014.

[3] M. Takakura, T. Matsumoto, M. Nakamura, Y. Mizumoto, S. Myojyo, R. Yamazaki, et al., "Detection of circulating tumor cells in cervical cancer using a conditionally replicative adenovirus targeting telomerase-positive cells," Cancer Sci, vol. 109, pp. 231-240, Jan 2018.

[4] Y. P. Yang, T. M. Giret, and R. J. Cote, "Circulating Tumor Cells from Enumeration to Analysis: Current Challenges and Future Opportunities," Cancers (Basel), vol. 13, May 31 2021.

[5] M. Qin, S. Chen, T. Yu, B. Escuadro, S. Sharma, and R. K. Batra, "Coxsackievirus adenovirus receptor expression predicts the efficiency of adenoviral gene transfer into non-small cell lung cancer xenografts," Clin Cancer Res, vol. 9, pp. 4992-9, Oct 15 2003.

[6] O. Ronneberger, P. Fischer, T. Brox, U-Net: Convolutional Networks for Biomedical Image Segmentation. Lect Notes Comput Sc 2015;9351:234-41.

[7] Z. Guo, X. Lin, Y. Hui, J. Wang, Q. Zhang, and F. Kong, "Circulating Tumor Cell Identification Based on Deep Learning," Front Oncol, vol. 12, p. 843879, 2022.

[8] Q. Liu, A. Junker, K. Murakami, and P. Hu, "Automated Counting of Cancer Cells by Ensembling Deep Features," Cells, vol. 8, Sep 2 2019.

[9] P.K. Saha, J.K. Udupa, D. Odhner, "Scale-based fuzzy connected image segmentation: Theory, algorithms, and validation," Computer Vision Image Understanding, Vol. 77, pp.145–174, 2000.

[10] U. Bagci, JK Udupa, X.J. Chen, "Ball-scale based hierarchical multi-object recognition in 3D medical images", SPIE Medical Imaging, Proc. SPIE 7623, Medical Imaging 2010: Image Processing, 762345 (12 March 2010); doi: 10.1117/12.839920.

Automatic Circulating Tumor Cell Segmentation and Enumeration in Digital Pathology by Using Deep Learning and Ball-scale Based Filtering Techniques

L. Tong[1] and Y. Wan[2]*

1. Conestoga High School, Berwyn, Pennsylvania, USA
2. Biomedical Engineering Department, Binghamton University, New York, USA

BIOMEDICAL ENGINEERING
BINGHAMTON UNIVERSITY

* - corresponding author

Background

- Circulating Tumor Cells (CTCs) detection currently uses expert cytopathologist screening to succeed.
- Heavy time cost and human labor for experts to continuously go through and check large amount of CTCs.
- Experts in both fields have looked for solutions, previous studies have used manual thresholding as a discriminator to detect CTCs with poor results.
- The B-scale filter utilizes a filtering method to return various information, such as sphericality and maximum radius that can be measured and useful for CTC counting.
- We investigated CTC counting by combining deep learning and prior human knowledge of CTCs from ball-scale (B-scale) filter and proposed an automatic CTC enumeration approach from the fluorescence images.

Purpose

- To create a U-Net Model which utilizes B-scale as a discriminator to behave like current expert cytopathologist behaviors in enumeration of CTCs.

Image Dataset

- PBMC (peripheral blood mononuclear cells) were extracted from cancerous patient blood, then were refined through infection by rAd^{CTC}, staining by anti-CD45 antibody, and DNA staining dye DAPI+.
- A total of 1137 fluorescence ground truth images were used to train, validate, and test our models.
- Ground truths were segmented twice in two different methods to account for the two different neural networks put to work here.
- Center-point based rectangles around positive CTC confirmed cells were drawn to train a ROI-obtaining network
- Ground truth segmented images of CTC cells themselves in a ROI concentrated region were then drawn to train a segmentation network that would be put into the enumeration discriminator.

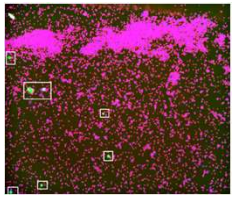

Figure 1. Rectangular ROI Ground Truth

Data sets	Detection	Segmentation	Enumeration
Training	233 images	236 images	198 images (323 CTCs)
Validation	93 images	95 images	
Testing	140 images	142 images	
Total	466 images	473 images	
Size	1280×1080×3	64×64×3	1280×1080×3

Table 1. Image Dataset

Methodology and Process

Flowchart

- The design that we picked was optimized to recreate the process in which screening was done through expert cytopathologists through studying processes and images.
- We identified two main steps: detection in which experts would find the general area of the CTC cell, and enumeration through segmentation by focusing in that given area and determining if that CTC cell is a true positive through an extra B-scale discriminator step.

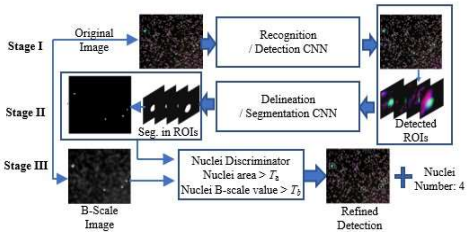

Figure 2. Framework of Experiment

Recognition

- Recognition/detection would result in a given area to search for the cell, resulting in increased success for enumeration through segmentation.
- The neural network was taught to recognize a specific boundary for CTC cells through center-point based ROI detection methods.
- The coordinates for all of the points of the rectangle and a probability map of the centers of the cells would be outputted.
- 466 images used to train for the Detection network, splitting [233:93:140] to train, validate, and test

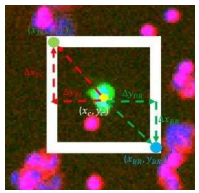

Figure 3. Center-point Based ROI Detection

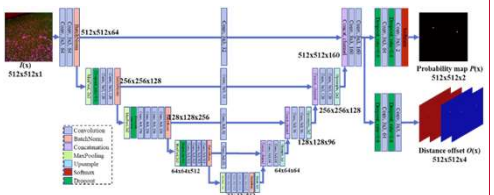

Figure 4. Recognition Network Architecture

Delineation

- Segmentation/delineation would result in a completely segmented cell mask
- Based on the selected ROI region, the computer would only segment in the selected area for the CTCs, thus becoming more efficient rather than spending time recognizing the CTC again
- 473 images used to train for Segmentation network, splitting [236:95:142] to train, validate, and test the segmentation network.

B-scale in Discriminator

- B-scale compared at the very end with the cell size taken into account to rule out any false positives that seem like cells but are not.
- Smaller cells can still react by overproducing but are not truly CTCs – B-scale gives us this advantage to enumerate these cells given past information known as size

Results and Conclusions

Results

- Figure A shows the untouched image before input into the neural network

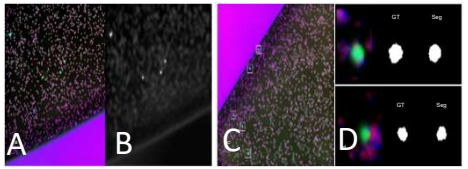

Figure 5. Summary of Results and Process

- Figure B shows the green channel of cells highlighted and normalized before being put into the recognition network
- Figure C shows the aftermath of the recognition network, with all of the rectangles and recognized ROIs
- Figure D shows the output of the segmentation network, with the masks on the right and the ground truth on the left
- The B-scale filter method was then used in the discriminator to further refine the results through homogeneity and feedback based on maximum ball radius (size)
- Using the testing images to test the validity and efficiency of the Detection and Segmentation networks we gathered the resulting numbers.

Methods	Detection		Segmentation	Enumeration
	Precision	Recall	DICE	Missing rate
Proposed	0.98/0.10	0.92/0.18	0.85/0.08	0.04
Threshold	0.82/0.15	0.96/0.13	0.69/0.14	0.30

Table 2. Precision and DICE for methods

- As seen, the proposed method with the B-scale filter acquired a precision of 0.98, and had a missing rate of 0.04
- Current methods using the threshold, which only differentiates based on intensity, had a missing rate of 0.30 and a precision of 0.82

Conclusions

- The proposed method was generally a success with comparable results to current in-use ones.
- While we tested a single rectangle based ROI, perhaps having a circular ROI similar to the ground truth for segmentation network could improve our numbers even further
- In addition, we could not get the ratio of negatives as getting ground truths for true negatives would be very difficult. However, our low level of false positives still is acceptable and makes our results competitive nonetheless.

Acknowledgements

This research was made possible by NCI grant #1R37255948.

Sources

1. S. J. Hao, et. al, "Size-based separation methods of circulating tumor cells," Adv Drug Deliv Rev, vol. 125, pp. 3-20, Feb 1 2018.
2. N. Aceto, et al., "Circulating tumor cell clusters are oligoclonal precursors of breast cancer metastasis," Cell, vol. 158, pp. 1110-1122, Aug 28 2014.
3. M. Takakura, et al., "Detection of circulating tumor cells in cervical cancer using a conditionally replicative adenovirus targeting telomerase- positive cells," Cancer Sci, vol. 109, pp. 231-240, Jan 2018.
4. Y. P. Yang, et al., "Circulating Tumor Cells from Enumeration to Analysis: Current Challenges and Future Opportunities," Cancers (Basel), vol. 13, May 31 2021.
5. M. Qin, et al., "Coxsackievirus adenovirus receptor expression predicts the efficiency of adenoviral gene transfer into non-small cell lung cancer xenografts," Clin Cancer Res, vol. 9, pp. 4992-9, Oct 15 2003.
6. O. Ronneberger, et al., U-Net: Convolutional Networks for Biomedical Image Segmentation. Lect Notes Comput Sc 2015;9351:234-41.
7. Z. Guo, et al., "Circulating Tumor Cell Identification Based on Deep Learning," Front Oncol, vol. 12, p. 843879, 2022.
8. Q. Liu, et. al, "Automated Counting of Cancer Cells by Ensembling Deep Features," Cells, vol. 8, Sep 2 2019.
9. P.K. Saha, J.K. Udupa, D. Odhner, "Scale-based fuzzy connected image segmentation: Theory, algorithms, and validation," Computer Vision Image Understanding, Vol. 77, pp.145–174, 2000.
10. U. Bagci, JK Udupa, X.J. Chen, "Ball-scale based hierarchical multi-object recognition in 3D medical images", SPIE Medical Imaging, Proc. SPIE 7623, Medical Imaging 2010: Image Processing, 762345 (12 March 2010); doi: 10.1117/12.839920.